

## Novel Cyclic Compounds as Potent Phosphodiesterase 4 Inhibitors

Wei He,\* Fu-Chih Huang, Barbara Hanney, John Souness, Bruce Miller, Guyan Liang, Jon Mason,<sup>†</sup> and Stevan Djuric<sup>‡</sup>

Department of Medicinal Chemistry, SW 8 Rhône-Poulenc Rorer Central Research, 500 Arcola Road, Collegeville, Pennsylvania 19426

Received August 28, 1997

The synthesis and biological activity of a novel series of 2,2-disubstituted indan-1,3-dione-based PDE4 inhibitors are described. This structurally unique class of PDE4 inhibitors is markedly different from the known PDE4 inhibitors such as RP 73401 (**2**) and CDP 840 (**3**). Structure–activity relationship (SAR) studies led to the identification of inhibitors with nanomolar potency and oral activity in a murine endotoxemia model for TNF- $\alpha$  inhibition. Unlike other classical PDE4 inhibitors, several analogues were found to be nonemetic in a canine emesis model at intravenous doses of up to 3 mg/kg.

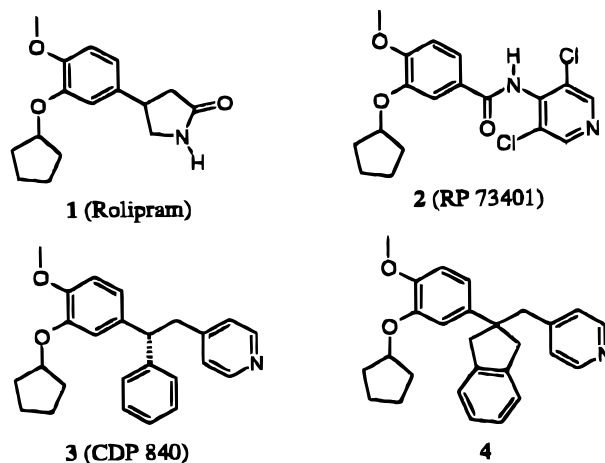
### Introduction

Tumor necrosis factor- $\alpha$  (TNF- $\alpha$ ) has been implicated in the pathogenesis of a number of autoimmune and inflammatory diseases including rheumatoid arthritis and sepsis.<sup>1</sup> Consequently, manipulation of the cytokine signaling or biosynthetic pathways associated with these proteins may provide therapeutic benefit in the above-mentioned disease states. It has been demonstrated that TNF- $\alpha$  production in proinflammatory cells becomes attenuated by an elevation of intracellular cyclic adenosine 3',5'-monophosphate (cAMP).<sup>2</sup> This second messenger is regulated by the phosphodiesterase (PDE) family of enzymes. Inhibition of one such enzyme, the calcium-independent and cAMP-specific PDE4, represents an attractive approach toward immunoinflammatory disease therapy.<sup>3</sup>

The prototype PDE4 inhibitor rolipram (**1**)<sup>4</sup> (Chart 1) exhibits several untoward side effects, which have precluded its clinical development as an antidepressant drug.<sup>5</sup> Most of the other PDE4 inhibitors<sup>3e,6b</sup> also possess side effects such as emesis; therefore, their therapeutic applications have been limited. PDE4 has been shown to have two binding sites for rolipram, consisting of a high-affinity site (Sr,  $K_i = 10$  nM) and a catalytic site (Sc,  $K_i = 300$  nM).<sup>7</sup> It has been suggested that some of the side effects are associated with the high-affinity binding site.<sup>8,6b–e,3e</sup> Recently, Warreilow et al. have disclosed a new class of inhibitors that display selectivity for Sc over Sr and claimed that no adverse effects in phase I human clinical trials were observed with the prototype inhibitor CDP 840 (**3**).<sup>9</sup> Overall, the mechanism responsible for the side effects of PDE4 inhibitors is still not well-understood.

RP 73401 (**2**) is a potent benzamide PDE4 inhibitor,<sup>6a</sup> which shows no selectivity for inhibiting PDE4 (catalytic site) over the displacement of rolipram from its binding site. The orientation of the aromatic groups in **2** is dependent on the amide linker as well as the dichloro substitution.<sup>6a</sup> In addition, it is conceivable that the amide bond can undergo hydrolysis, and thus undesir-

Chart 1



able metabolites might be generated. It was decided to replace the amide linker of **2** with a conformationally constrained indan ring linker which cannot be cleaved. The indan ring in the initial template (**4**) dictated the orientation of the pyridyl and 4-methoxy-3-cyclopentoxyphenyl rings. Since PDE4 has been shown to have two different binding sites for rolipram, substitutions on the aromatic ring of indan with functional groups could provide different interactions (through hydrogen bonding and van der Waals forces). In contrast, the benzamide-type PDE4 inhibitors such as **2**<sup>6a,9d</sup> cannot engage in such interactions. Our ultimate goals were to discover PDE4 inhibitors that maintain antiinflammatory properties but with reduced side effects and to assess the role of selectivity of the catalytic over high-affinity binding sites in contributing to the side effects.

Several conformational studies of **1** and its analogues have been published.<sup>6f,g</sup> However, it is not feasible to use molecular modeling to study the interaction of PDE4 and its inhibitors since neither the three-dimensional structure of PDE4 nor its homology model is available. Molecular modeling was applied for the analysis of conformational overlaps of target compounds and **2**. It was used as a tool to select target compounds for synthesis and was not used to interpret structure–activity relationships (SAR) in detail. A superposition

<sup>†</sup> Current address: Bristol-Myers Squibb, Princeton, NJ.

<sup>‡</sup> Current address: Abbott Laboratories, Abbott Park, IL.

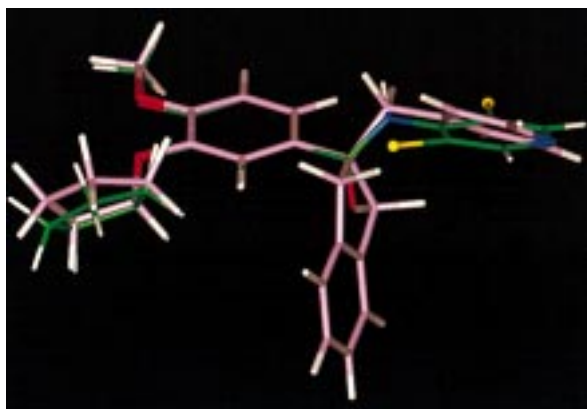


**Figure 1.** Superposition of low-energy conformations of indan **4** (purple) and **2** (green).

of low-energy conformations (from MOPAC/AM1 optimizations) of **2** and indan **4** is shown in Figure 1. The pyridine nitrogens are in very similar positions for both compounds, and the aromatic rings can also be in similar planes. Molecular modeling studies on **2** (MOPAC/AM1 calculations) found a series of structures with lowest energy where the bulky nature of the ortho substituents forces the aromatic ring and the amide group out of planarity. The X-ray structure<sup>10</sup> of the norbornyl (replacing cyclopentyl) analogue of **2** had a conformation similar to one of these MOPAC/AM1 low-energy conformers. This shows that both aromatic rings are out of conjugation with the amide bond and that the final conformations are practically equienergy. The carbonyl group faces in the same or opposite direction to the cyclopentyloxy substituent (up or down), and the *o*-dichloropyridyl ring ends up being at about 90° to the other aromatic ring (as shown in Figures 1–4). It can be noted that unlike for the **2** analogue, the indan **4** derivative does not require a dichloropyridyl ring to have such a low-energy conformation. It is in this context that we report upon the identification and biological profiles of a structurally unique class of cyclic PDE4 inhibitors.

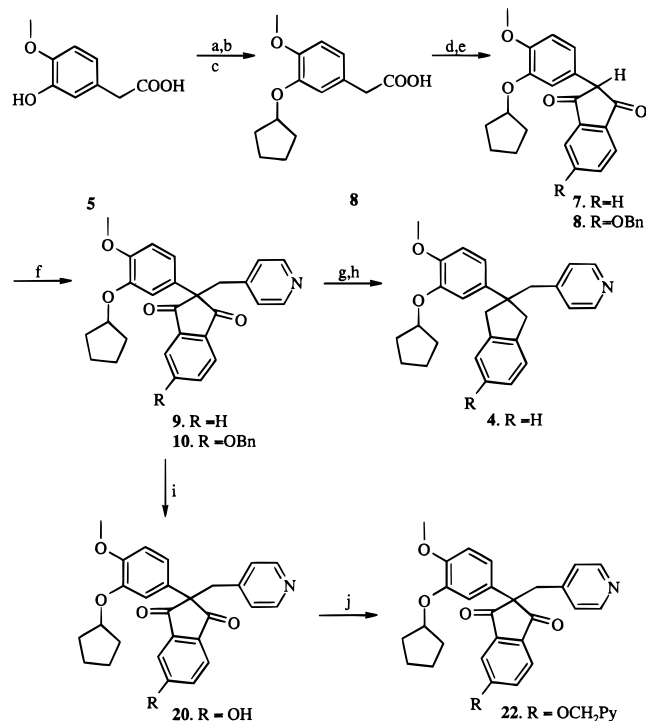
## Chemistry

The synthesis of the cyclic compounds is exemplified in Scheme 1. Acid **6** was obtained from commercially available 3-hydroxy-4-methoxyphenylacetic acid via esterification, Mitsunobu reaction<sup>11</sup> with cyclopentanol, and saponification. Gabriel-modified Perkin reaction<sup>12</sup> of acid **6** and various phthalic anhydrides afforded the monosubstituted indan-1,3-diones **7** and **8** which were then alkylated with 4-picolyl chloride. Selective hydrogenation of the 2,2-disubstituted indan-1,3-dione **10** delivered phenol **20** which was a versatile intermediate for further transformations. Reduction of indan-1,3-dione **9** into the corresponding indan **4** was achieved with sodium borohydride followed by triethylsilane/TFA.

## Biological Results and Discussion

The PDE4 inhibition and rolipram displacement data are summarized in Tables 1–3. The initial target compound **4**, as shown in Table 1, proved to be a rather weak PDE4 inhibitor with an IC<sub>50</sub> of 750 nM despite its structural resemblance to **3** (IC<sub>50</sub> of 7 nM).<sup>9</sup> The monosubstituted indan-1,3-dione intermediate **7** did not display any significant PDE4 inhibitory activity at

## Scheme 1. Synthesis of the Cyclic Compounds<sup>a</sup>



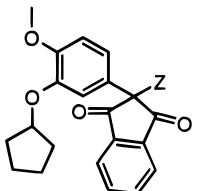
<sup>a</sup> (a) MeOH/H<sub>2</sub>SO<sub>4</sub> (98% yield); (b) DEAD/Ph<sub>3</sub>P/cyclopentanol (89% yield); (c) NaOH/MeOH, HCl (95% yield); (d) phthalic anhydride/NaOAc/heat; (e) NaOMe/MeOH, HCl (78% yield over two steps for **7** and 45% for **8**); (f) K<sub>2</sub>CO<sub>3</sub>/NaI/4-picolyl chloride (85% yield); (g) NaBH<sub>4</sub>/MeOH; (h) Et<sub>3</sub>SiH/TFA (90% yield over two steps for **4**); (i) 10% Pd/C/AcOEt (100% yield); (j) DEAD/Ph<sub>3</sub>P/4-pyridinylcarbinol (38% yield).

**Table 1.** Effects of Carbonyl Groups of the Cyclic Compounds

compd	X	Y	R	IC <sub>50</sub> (PDE4, nM) <sup>a,b</sup>	K <sub>i</sub> (rolipram bind, nM) <sup>b,c</sup>
<b>2</b>				1	1
<b>4</b>	H,H	H,H	H	750	1600
<b>9</b>	O	O	H	30	10
<b>16</b>	H,OH	H,OH	H	> 10000	> 10000
(+)- <b>10</b>	O	O	benzyloxy	4	20
(-)- <b>17</b>	O	O	benzyloxy	6	20
(+)- <b>18</b>	O	O	benzyloxy	30	20
<b>19</b>	H,H	O	benzyloxy	20	60

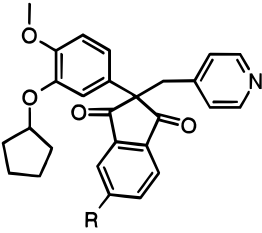
<sup>a</sup> IC<sub>50</sub> and K<sub>i</sub> values were determined from concentration–response curves (*n* = 3) in which concentrations ranged from 0.1 nM to 10 μM. Errors were within ±20%. <sup>b</sup> PDE activity was determined in macrophage homogenates by the two-step radioisotopic method of Thompson et al.<sup>18</sup> <sup>c</sup> (±)-[<sup>3</sup>H]Rolipram binding assays were performed using guinea pig brain membranes as described by Schneider et al.<sup>8b</sup>

concentrations up to 10 μM (Table 2). However, several alkylation products derived from **7** demonstrated increased potency (e.g., **9**, **13**, and **15**). The precursor indan-1,3-dione **9** had much better inhibitory activity (IC<sub>50</sub> of 30 nM, still less potent than **2**) than indan **4**. The initial approach based on indan **4** was abandoned,

**Table 2.** Effects of Alkylation of the Cyclic Compounds


compd	Z	IC <sub>50</sub> (PDE4, nM) <sup>a,b</sup>	K <sub>i</sub> (rolipram bind, nM) <sup>b,c</sup>
<b>2</b>		1	1
<b>7</b>	H	>10000	>10000
<b>9</b>	pyridin-4-ylmethyl	30	10
<b>12</b>	phenylmethyl	500	2300
<b>13</b>	4-hydroxyphenylmethyl	70	260
<b>14</b>	3,5-dichloropyridin-4-ylmethyl	3000	1700
<b>15</b>	1-oxypyridin-4-ylmethyl	50	20

<sup>a</sup> IC<sub>50</sub> and K<sub>i</sub> values were determined from concentration–response curves (*n* = 3) in which concentrations ranged from 0.1 nM to 10 μM. Errors were within ±20%. <sup>b</sup> PDE activity was determined in macrophage homogenates by the two-step radioisotopic method of Thompson et al.<sup>18</sup> <sup>c</sup> (±)-[<sup>3</sup>H]Rolipram binding assays were performed using guinea pig brain membranes as described by Schneider et al.<sup>8b</sup>

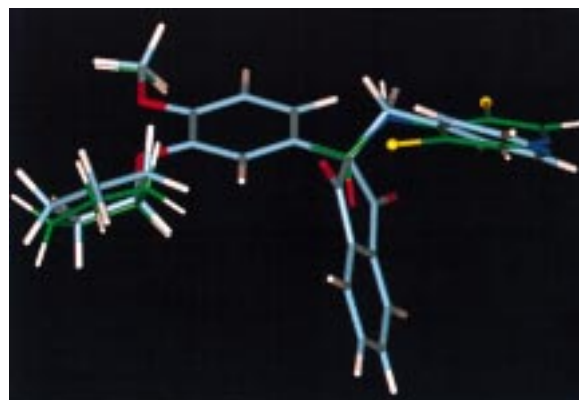
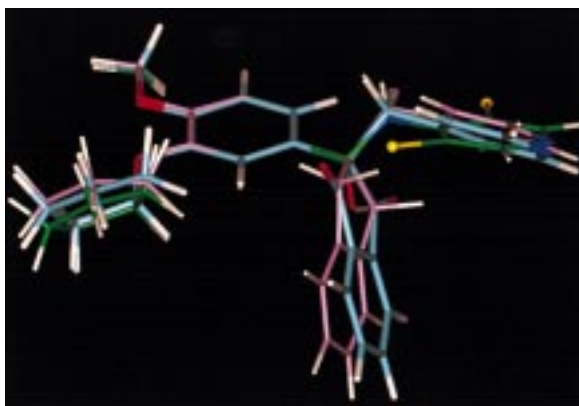
**Table 3.** Effects of Substitution on the Indan Ring of the Cyclic Compounds


compd	R	IC <sub>50</sub> (PDE4, nM) <sup>a,b</sup>	K <sub>i</sub> (rolipram bind, nM) <sup>b,c</sup>
<b>2</b>		1	1
<b>9</b>	H	30	10
<b>10</b>	benzyloxy	4	20
<b>20</b>	OH	100	45
<b>21</b>	ethoxy	12	20
<b>22</b>	4-pyridinylmethoxy	14	30
<b>23</b>	carboxymethoxy	50	20
<b>24</b>	1-methylpiperidin-4-ylxy	30	60
<b>25</b>	[1,4']-bipiperidinyl-1'-carbonyloxy	30	20

<sup>a</sup> IC<sub>50</sub> and K<sub>i</sub> values were determined from concentration–response curves (*n* = 3) in which concentrations ranged from 0.1 nM to 10 μM. Errors were within ±20%. <sup>b</sup> PDE activity was determined in macrophage homogenates by the two-step radioisotopic method of Thompson et al.<sup>18</sup> <sup>c</sup> (±)-[<sup>3</sup>H]Rolipram binding assays were performed using guinea pig brain membranes as described by Schneider et al.<sup>8b</sup>

and indan-1,3-dione **9** was used as the initial lead compound from which the novel series of PDE4 inhibitors was developed. Although it was more selective than compound **9** (Table 2), subsequently synthesized phenol **13** was not pursued further because the results below seemed to indicate that the selectivity was not as critical as anticipated.

The data presented in Table 2 suggested that inhibitory potency was associated with the presence of functional groups capable of forming hydrogen bond interactions with the enzyme (e.g., pyridyl and phenol groups). A superposition of a low-energy structure of

**Figure 2.** Superposition of low-energy conformations of **2** (green) and indan-1,3-dione **9** (light blue).**Figure 3.** Superposition of low-energy conformation of indan-1,3-dione **9** (light blue), indan **4** (purple), and **2** (green).

the indan-1,3-dione **9** with **2** is shown in Figure 2, together with indan **4** in Figure 3. The overlap of the position and directionality of the nitrogens of pyridines can be clearly seen, and the common region for potential interaction of a chlorine atom on **2** and carbonyl oxygen on indan-1,3-dione **9** can also be noted. In addition, the indan-1,3-dione ring of compound **9** is slightly shifted away from the indan ring of compound **4**. This shift, in part, might account for the potency difference between compounds **4** and **9** (Table 1). The poor activity of the dichloropyridine analogue **14** in Table 2 was not surprising because steric interactions of the bulky chlorine atoms with the indan-1,3-dione ring destabilize conformations where the pyridine ring nitrogen can overlap with that of **2**. A superposition of a low-energy structure of **14** with **2** is shown in Figure 4. This result clearly distinguishes the cyclic compounds from the benzamide class of PDE4 inhibitors where the dichloropyridine analogue **2** is the most potent compound in that series.<sup>6a</sup> The dichloro analogue of indan **4** was not pursued due to the poor activities of indan **1** and indan-1,3-dione **14**.

Indan **4** was about 750-fold less potent than **2** as a PDE4 inhibitor despite good conformational overlaps according to molecular modeling. This observation is understandable since the conformational modeling does not take other interactions into account. The indan ring of compound **4** might have unfavorable steric interaction with PDE4 and thus destabilize the overall interaction of compound **4** with PDE4. Furthermore, **2** is a much more rigid molecule than compound **4**, and its amide bond might also provide additional interactions with

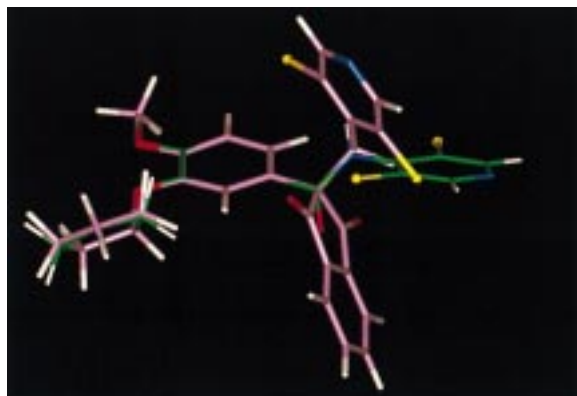


**Figure 4.** Superposition of low-energy conformation of indan-1,3-dione **14** (purple) and **2** (green). The chlorines force a different low-energy conformation; the conformation with the pyridine in the same position as **2** is sterically hindered.

PDE4. The potency improvement from indan **4** to indan-1,3-dione **9** could result from the previously mentioned ring shift and/or additional bonding from the carbonyl groups to PDE4.

Further potency enhancements were achieved through functionalization of the aromatic ring of the indan-1,3-dione. The benzyloxy derivative **10** with an  $IC_{50}$  of 4 nM proved to be the most potent inhibitor of PDE4 within this series synthesized so far (Tables 1 and 3). The fact that compound **10**, capable of interacting with an additional binding site, is less potent than **2** in the PDE4 assay seems to indicate there is still room for potency improvement of the cyclic series. The conformational freedom of compound **10** and perhaps the different binding mode of the cyclic inhibitors with PDE4 might account for the potency difference between **2** and indan-1,3-dione **10**. Interestingly, the corresponding indanone **19** (stereochemistry not confirmed) also retained good potency. The carbonyl groups in **10** and **19** clearly had a significant effect on the inhibitory potency. Whether the effect of the carbonyl groups is steric or electronic in nature remains to be ascertained. Racemic **10** was resolved by chiral HPLC to afford the (–)-enantiomer **17** and the (+)-enantiomer **18** (absolute stereochemistry not determined) with the former being 5-fold more potent against PDE4. Interestingly, the two enantiomers were equipotent in displacing rolipram from the high-affinity binding site.

As exemplified in Table 3, substitutions on the aromatic ring of the indan-1,3-dione proved to be reasonably well-tolerated. The selectivity profiles of the cyclic PDE4 inhibitors were not affected by the nature of substituents, ranging from acidic to basic and from small to bulky. These observations allowed us to use this site as a handle for modification to identify compounds with improved pharmacodynamic and pharmacokinetic profiles relative to the initial lead compound **9** (discussion below). This observation also seemed to indicate that additional pockets in the active site might exist and that these need to be explored further.

The initial lead compound **9** was shown to have good inhibitory potency against TNF- $\alpha$  release from human mononuclear cells stimulated with LPS<sup>13</sup> with  $IC_{50}$  of 0.2  $\mu$ M, comparable with **1** ( $IC_{50}$  of 0.5  $\mu$ M).<sup>13c</sup> Several compounds from the cyclic series were selected for further evaluation as potential antiinflammatory agents.

**Table 4.** Effects of **1**, **3**, **9**, **10**, and **25** in the Murine Endotoxemia Model

compd	$IC_{50}$ of TNF- $\alpha$ inhibition ( $\mu$ M) <sup>a</sup>	$ED_{50}$ or % of TNF- $\alpha$ inhibition (mg/kg/po) <sup>b</sup>
<b>1</b>	0.5	8
<b>3</b>		25
<b>9</b>	0.2	0% @ 30
<b>10</b>	0.2	40% @ 30
<b>25</b>		15

<sup>a</sup>  $IC_{50}$  values were determined from concentration–response curves ( $n = 3$ ) in which concentrations ranged from 0.1 nM to 10  $\mu$ M. Errors were within  $\pm 20\%$ . <sup>b</sup>  $ED_{50}$  values were determined from dose–response curves of TNF- $\alpha$  inhibition. Compounds were administered orally to mice 4 h prior to LPS challenge.

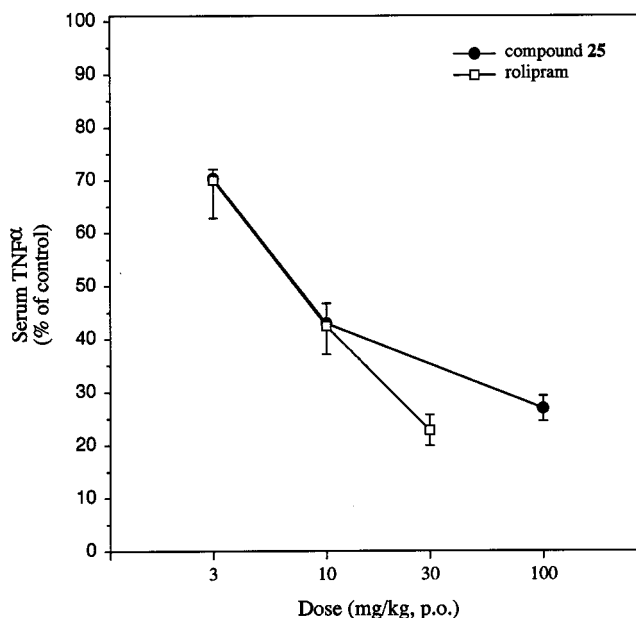


**Figure 5.** Dose–response curves of TNF- $\alpha$  inhibition for compound **25** and rolipram. Compounds were administered orally to mice 4 h prior to LPS challenge. Results are means  $\pm$  SEM ( $n = 6$  animals/group).

They were tested in a murine endotoxemia model via inhibition of TNF- $\alpha$  release (Table 4). To identify long-acting antiinflammatory agents and to differentiate PDE4 inhibitors within the series, the murine endotoxemia model was developed with the oral administration of test compounds 4 h prior to LPS challenge, very different from those reported in the literature where compounds were given 30 min before LPS injection.<sup>13b</sup> For comparison, **1** was shown to have an  $ED_{50}$  of 8 mg/kg/po in the murine endotoxemia model, while its  $ED_{50}$  was reported to be less than 3 mg/kg/po in a similar model.<sup>13b</sup> The initial lead compound **9** was found to be inactive in the murine endotoxemia model, while the more potent analogue **10** demonstrated 40% inhibition of TNF- $\alpha$  release at 30 mg/kg/po. This result was not surprising since both compounds **9** and **10** were very lipophilic (with log  $P$  values of 5.5 and 5.96, respectively), and their bioavailability might be poor. **3** was found to have an  $ED_{50}$  of 25 mg/kg/po in the same in vivo assay. Compound **25**, with the incorporation of nitrogen atoms to increase its polarity and water solubility, exhibited an  $ED_{50}$  of 15 mg/kg/po in a murine endotoxemia model (Figure 5). On the molar basis compound **25** was equipotent to rolipram in the model since its molecular weight is more than twice that of rolipram.

**Table 5.** Results of Dog Emesis Studies

compd	dose tested (mg/kg/iv)	ratio of emetic dogs/total dogs
vehicle (DMSO)		0/3
<b>1</b>	0.01	1/2
	0.03	2/2
	0.2	2/2
<b>2</b>	0.6	4/4
	1	0/4
<b>10</b>	0.7	0/4
	3	0/4
<b>25</b>	3	0/4

To evaluate the most common side effects, a dog emesis model was chosen because dogs are the most sensitive species to emesis. The intravenous administration was applied to achieve initial high plasma concentration of compounds and to ensure that compounds tested were in the circulation. Thus, cross-species difference such as oral bioavailability could be avoided since efficacy and emesis studies were conducted in two different species (mouse and dog). Interestingly, no emesis was observed with any of four dogs when indan-1,3-diones **10** and **25** were given at doses up to 3 mg/kg/iv, while administration with rolipram caused emetic symptoms even at a dose of 0.01 mg/kg/iv with one out of two dogs (Table 5). Two out of two dogs were observed to have emetic symptoms when **1** was administered at doses of 0.03 and 0.2 mg/kg/iv. Intravenous administration of **2** at a dose of 0.6 mg/kg also resulted in emesis with four out of four dogs.<sup>14</sup>

From the data presented above, we have identified a novel series of inhibitors that display reasonable PDE4 inhibitory activity with certain members also showing reduced rolipram binding affinity compared with **2**. The data does not demonstrate any correlation between PDE4 inhibition and rolipram binding displacement. More importantly, both **10** and **25** were still nonemetic at the doses tested despite having different ratios for the catalytic/rolipram binding affinity, which seems to raise questions about the hypothesis concerning the role of selectivity or the catalytic/rolipram binding sites in their contribution to the side effects. It is also possible that **10** and **25** cannot penetrate into the brain,<sup>15</sup> although some compounds do not have to cross the blood-brain barrier to cause emesis. It has not been determined what effects compounds **10** and **25** will have at doses higher than 3 mg/kg/iv in the emesis studies. Additional studies are needed to address these issues. Nevertheless, we have identified PDE4 inhibitors with improved therapeutic windows as indicated by the inhibitory dose of TNF- $\alpha$  release and the no-effect dose of emesis.

## Conclusions

In summary, we have elaborated a structurally novel class of indan-1,3-dione-based PDE4 inhibitors with reasonable (nanomolar) potencies in a PDE4 assay. This series of PDE4 inhibitors is clearly different from the known PDE4 inhibitors such as **2** and **3**. The carbonyl groups of the indandione or indanone compounds were critical for the inhibitory activities. The indan ring could be substituted to improve the PDE4 inhibitory activity, and substitutions on this part of the molecules did not affect selectivity. This region of the cyclic

compounds was identified as a handle to improve the pharmacodynamic and pharmacokinetic profiles of the cyclic PDE4 inhibitors. The tolerance of substitutions in such a region of the cyclic compounds seems to suggest that there might be a pocket in the active site of PDE4 which has not been explored by the known PDE4 inhibitors such as **2** and **3**, and this could be exploited further in the future. In addition, some of these cyclic compounds were found to be orally active in a murine endotoxemia model via TNF- $\alpha$  inhibition. Significantly, two of these compounds (**10** and **25**) were shown to have no emetic activity in a dog model at intravenous doses up to 3 mg/kg. Further studies on this interesting class of PDE4 inhibitors are in progress.

## Experimental Section

**Chemistry.** Representative syntheses of the target compounds are shown below. All final compounds were characterized by melting point, <sup>1</sup>H NMR, mass spectra, and elemental analyses. Some of compounds were hygroscopic and amorphous, as noted below for each compound. Melting points of such amorphous solids were taken on a Thomas-Hoover (Uni-Melt) capillary melting point apparatus and are uncorrected. Elemental analyses were performed by QTI, Whitehouse, NJ. The concentration of hygroscopic compounds for biological evaluation was calculated based on the hydrated formula weight derived from elemental analyses. <sup>1</sup>H NMR spectra were recorded on a Bruker AC 300 spectrometer. Mass spectra were measured on Finnigan 4500 or VG 70 SE instruments. Flash chromatography was conducted with 230–400 mesh silica gel (EM Science). Optical rotations were recorded on a Perkin-Elmer 241 polarimeter. Reagents were used as received from commercial suppliers.

**4-Methoxy-3-(cyclopentyloxy)phenylacetic Acid (6).** To a solution of 3-hydroxy-4-methoxyphenylacetic acid (10 g, 55 mmol) in 50 mL of anhydrous methanol was added 1 mL of concentrated sulfuric acid, and the resulting mixture was refluxed for 2 h before being concentrated to dryness. The residue was redissolved in 100 mL of ether; the organic layer was washed with saturated sodium bicarbonate and then dried over magnesium sulfate. Filtration and concentration provided 10.6 g (98%) of the corresponding methyl ester as an oil.

The above ester was dissolved in 20 mL of THF and at room temperature treated with cyclopentyl alcohol (5 g, 58 mmol), triphenylphosphine (17 g, 65 mmol), and DEAD (11.3 g, 65 mmol), and the resulting brown solution was stirred overnight. After being concentrated to dryness, the residue was diluted with 100 mL of ether, and solids were removed by filtration. The residue obtained by concentration was purified by chromatography on silica gel (30% ether/hexane) to give 12.6 g (89%) of a liquid.

The above liquid was treated with 60 mL of methanol and 60 mL of 1 N sodium hydroxide, and the mixture was vigorously stirred at room temperature overnight. The aqueous solution after removal of methanol was acidified with 1 N hydrochloric acid. The solid was collected by filtration and then dried under high vacuum to afford 11.4 g (95%) of the desired acid.

**2-(3-(Cyclopentyloxy)-4-methoxyphenyl)indan-1,3-dione (7).** **General Procedure 1:** A mixture of 4-methoxy-3-(cyclopentyloxy)phenylacetic acid (2.5 g, 10 mmol), phthalic anhydride (4.5 g, 30 mmol), and sodium acetate (1 g, 12 mmol) was heated at 200 °C for 4 h and then cooled to room temperature before being dissolved in 100 mL of dichloromethane. The organic phase was washed with saturated sodium bicarbonate (100 mL) and dried over magnesium sulfate. The residue obtained by filtration and concentration was redissolved in 20 mL of methanol before being treated with a 25% sodium methoxide/methanol solution (6.9 mL). The reddish suspension was refluxed for 0.5 h and then concentrated to dryness. The residue was acidified with concentrated

hydrochloric acid at 0 °C and then extracted with dichloromethane (3 × 50 mL). The organic layer was dried over magnesium sulfate and then filtered. The solution was concentrated to give the indan-1,3-dione (2.62 g, 78%): yellow solid; mp 128–130 °C; MS *m/z* 336 ( $M^+$ ). Anal. ( $C_{21}H_{20}O_4$ ) C, H.

**6-(Benzyloxy)-2-(3-(cyclopentylloxy)-4-methoxyphenyl)indan-1,3-dione (8).** A mixture of 4-(benzyloxy)phthalic anhydride<sup>16</sup> (4.50 g, 18.5 mmol), triethylamine (13 mL, 93.3 mmol), 3-(cyclopentylloxy)-4-methoxyphenylacetic acid (4.63 g, 18.5 mmol), and acetic anhydride (10 mL) was heated to reflux for a total of 4 h. The mixture was concentrated to yield a thick black tar which was dissolved in dichloromethane (100 mL) and then poured into ice water (200 mL). The organic phase, after washing with water, was dried with magnesium sulfate. The crude material obtained by filtration and concentration was dissolved in methanol before the addition of 25% sodium methoxide in methanol (30 mL). The resulting reaction mixture was refluxed for 1 h and then worked up as above to give 3.7 g (45%) of the corresponding indan-1,3-dione: light-yellow solid; hygroscopic; MS *m/z* 442 ( $M^+$ ). Anal. ( $C_{28}H_{26}O_5 \cdot 0.2H_2O$ ) C, H.

**2-(3-(Cyclopentylloxy)-4-methoxyphenyl)-2-(pyrid-4-ylmethyl)indan-1,3-dione (9).** **General Procedure 2:** A suspension of **7** (1.34 g, 4.0 mmol), potassium carbonate (1.5 g), sodium iodide (300 mg), and 4-picoyl chloride hydrochloride (800 mg, 4.8 mmol) in 30 mL of acetone was refluxed for 1 h and then diluted with ether (50 mL) at room temperature. The residue obtained by filtration and concentration was purified by chromatography on silica gel (50% ether/hexane) to give 1.25 g (73%) of the desired product: yellow solid; mp 154–155 °C; MS *m/z* 427 ( $M^+$ ). Anal. ( $C_{27}H_{25}NO_4$ ) C, H, N.

**4-[2-(3-(Cyclopentylloxy)-4-methoxyphenyl)indan-2-ylmethyl]pyridine (4).** To a solution of **9** (270 mg, 0.63 mmol) in methanol at room temperature was added sodium borohydride (100 mg, 2.6 mmol). The resulting suspension was stirred at room temperature for 1 h before being concentrated to dryness. The residue was treated with trifluoroacetic acid (4 mL) and triethylsilane (4 mL). The resulting mixture was stirred vigorously overnight before being diluted with dichloromethane (100 mL) and then washed with saturated sodium bicarbonate (50 mL). The organic phase was dried over magnesium sulfate and then filtered. The residue obtained by concentration was purified by chromatography on silica gel (30% ether/hexane) to give 225 mg (90%) of compound **4**: colorless oil; MS *m/z* 399 ( $M^+$ ). Anal. ( $C_{27}H_{29}NO_2$ ) C, H, N.

**6-(Benzyloxy)-2-(3-(cyclopentylloxy)-4-methoxyphenyl)-2-(pyrid-4-ylmethyl)indan-1,3-dione (10).** Compound **10** was prepared according to general procedure 2 starting with **8** and purified by chromatography on silica gel (50% ether/hexane): 202 mg (85% yield); yellow solid; mp 65–68 °C; MS *m/z* 533 ( $M^+$ ); <sup>1</sup>H NMR ( $CDCl_3$ )  $\delta$  8.32 (bd, 2H), 7.81 (d, 1H), 7.48–7.31 (bm, 7H), 7.11 (bd, 3H), 7.05 (bd, 1H), 6.85 (dd, 1H), 6.77 (d, 1H), 5.13 (s, 2H), 4.77 (m, 1H), 3.80 (s, 3H), 3.48 (s, 2H), 1.96–1.63 (m, 7H). Anal. ( $C_{34}H_{31}NO_5$ ) C, H, N.

**2-Benzyl-(3-(cyclopentylloxy)-4-methoxyphenyl)indan-1,3-dione (12).** Compound **12** was prepared according to general procedure 2: yellow solid; mp 116–119 °C; 53% yield; MS *m/z* 426 ( $M^+$ ). Anal. ( $C_{28}H_{26}O_4$ ) C, H.

**4-[2-(3-(Cyclopentylloxy)-4-methoxyphenyl)-1,3-dioxoindan-2-ylmethyl]phenyl Acetate.** The title intermediate of compound **13** was prepared according to general procedure 2: yellow solid; mp 130–132 °C; 74% yield; MS *m/z* 484 ( $M^+$ ). Anal. Calcd for  $C_{30}H_{28}O_6$ : C, 74.36; H, 5.82. Found: C, 74.01; H, 5.95.

**2-(3-(Cyclopentylloxy)-4-methoxyphenyl)-2-(4-hydroxybenzyl)indan-1,3-dione (13).** To a solution of 4-[2-(3-(cyclopentylloxy)-4-methoxyphenyl)-1,3-dioxoindan-2-ylmethyl]phenyl acetate (280 mg, 0.58 mmol) in 10 mL of methanol at 0 °C was added a 25% sodium methoxide/methanol solution (0.15 mL, 0.67 mmol). The resulting reddish solution was stirred at room temperature for 2 h before being concentrated to dryness and then acidified with 1 N hydrochloric acid. The acidified mixture was extracted with dichloromethane (2 × 50

mL) and then concentrated by rotary evaporation. The residue was purified by chromatography on silica gel (50% ethyl acetate/hexane) to give 192 mg (75%) of the desired product: yellow solid; hygroscopic; mp 172–173 °C; MS *m/z* 443 ( $M^+$  + 1). Anal. ( $C_{28}H_{26}O_5 \cdot 0.5H_2O$ ) C, H.

**2-(3-(Cyclopentylloxy)-4-methoxyphenyl)-2-(3,5-dichloropyrid-4-ylmethyl)indan-1,3-dione (14).** Compound **14** was prepared according to general procedure 2: yellow solid; mp 124–126 °C; 98% yield; MS *m/z* 496 ( $M^+$  + 1). Anal. ( $C_{27}H_{23}Cl_2NO_4$ ) C, H, N.

**2-(3-(Cyclopentylloxy)-4-methoxyphenyl)-2-(1-oxopyrid-4-ylmethyl)indan-1,3-dione (15).** To a solution of **9** (400 mg, 0.94 mmol) in 4 mL of dichloromethane at room temperature was added MCPBA (74%, 300 mg, 1.3 mmol). The resulting suspension was stirred at room temperature for 2 h before being quenched with a saturated solution of sodium bisulfite (1 mL). After being washed with 1 N sodium hydroxide (5 mL), the organic phase was concentrated, and the residue was purified by chromatography on silica gel (ethyl acetate) to afford 400 mg (96%) of the desired product: yellow solid; mp 215–217 °C; MS *m/z* 443 ( $M^+$ ). Anal. ( $C_{27}H_{25}NO_5$ ) C, H, N.

**2-(3-(Cyclopentylloxy)-4-methoxyphenyl)-2-(pyrid-3-ylmethyl)indan-1,3-diol (16).** To a solution of **9** (370 mg, 0.87 mmol) in 10 mL of THF at 0 °C was added a 1 M LAH/THF solution (1.7 mL, 1.7 mmol), and the mixture was stirred for 3 h before being quenched with 1 N hydrochloric acid and then neutralized to pH 7. The mixture was extracted with dichloromethane (2 × 50 mL). The residue obtained by concentration was purified by chromatography on silica gel (60% ethyl acetate/hexane) to give 277 mg (74%) of a mixture of diols: white solid; hygroscopic; mp 99–101 °C; MS *m/z* 432 ( $M^+$ ). Anal. ( $C_{27}H_{29}NO_4 \cdot 0.5H_2O$ ) C, H, N.

**(-)-6-(Benzyloxy)-2-(3-(cyclopentylloxy)-4-methoxyphenyl)-2-(pyrid-4-ylmethyl)indan-1,3-dione (17).** Compound **17** was resolved by chiral HPLC from racemic **10** (CHIRACEL OD) eluted with heptane/ethanol containing 0.1% diethylamine (1:3, v/v) detected at UV 230 nm at flow rate of 1 mL/min: retention time 6.5 min; yellow solid; mp 58–61 °C; MS *m/z* 533 ( $M^+$ );  $[\alpha]_D -8.8^\circ$  ( $c = 0.17, CHCl_3$ ).

**(+)-6-(Benzyloxy)-2-(3-(cyclopentylloxy)-4-methoxyphenyl)-2-(pyrid-4-ylmethyl)indan-1,3-dione (18).** Compound **18** was obtained with a retention time of 9.3 min: yellow solid; mp 55–60 °C; MS *m/z* 533 ( $M^+$ );  $[\alpha]_D +10^\circ$  ( $c = 0.17, CHCl_3$ ).

**5-(Benzyloxy)-2-(3-(cyclopentylloxy)-4-methoxyphenyl)-2-(pyrid-4-ylmethyl)indan-1-one (19).** A suspension of 4-[6-(benzyloxy)-2-(3-(cyclopentylloxy)-4-methoxyphenyl)indan-2-ylmethyl]pyridine (100 mg, 0.2 mmol, obtained from reduction of **10**) and 2,2'-bipyridinium chlorochromate (584 mg, 2 mmol) in 20 mL of acetone was refluxed overnight before being diluted with ether (100 mL) at room temperature. The mixture was filtered, washed with a saturated solution of copper(II) sulfate, and then concentrated. The residue was purified by chromatography on silica gel (50% ether/hexane) to give 25 mg (25%) of the title compound: white solid; mp 52–55 °C; MS *m/z* 520 ( $M^+$ ).

**2-(3-(Cyclopentylloxy)-4-methoxyphenyl)-5-hydroxy-2-(pyrid-4-ylmethyl)indan-1,3-dione (20).** A suspension of **10** (200 mg, 0.38 mmol) in 10 mL of ethyl acetate containing 200 mg of Pd/C (10%) was stirred at room temperature with a hydrogen balloon for 2 h before the Pd/C was removed by filtration. Concentration afforded 165 mg (100%) of compound **20**: yellow solid; hygroscopic; mp 106–109 °C; MS *m/z* 443 ( $M^+$ ). Anal. ( $C_{27}H_{25}NO_5 \cdot 0.5H_2O$ ) C, H, N.

**2-(3-(Cyclopentylloxy)-4-methoxyphenyl)-5-(pyridin-4-ylmethoxy)-2-(pyridin-4-ylmethyl)indan-1,3-dione (22).** A mixture of **20** (140 mg, 0.32 mmol), 4-pyridinylcarbinol (140 mg, 1.28 mmol), triphenylphosphine (335 mg, 1.28 mmol), and DEAD (0.2 mL, 1.28 mmol) in 10 mL of THF was stirred at room temperature overnight. After being concentrated to dryness, the residue was purified by chromatography on silica gel (ethyl acetate) to give 65 mg (38%) of the desired product: yellow solid; hygroscopic; mp 67–70 °C; MS *m/z* 534 ( $M^+$ ); <sup>1</sup>H NMR ( $CDCl_3$ )  $\delta$  8.65 (d, 1H), 8.6 (d, 1H), 8.6 (d, 2H), 7.86 (d,

1H), 7.37–7.21 (m, 5H), 7.1 (s, 1H), 7.05 (d, 1H), 6.95–6.89 (bd, 1H), 6.78 (d, 1H), 5.16 (s, 2H), 4.75 (m, 1H), 3.78 (s, 3H), 3.49 (s, 2H), 1.96–1.63 (m, 3H). Anal. (C<sub>27</sub>H<sub>25</sub>NO<sub>5</sub>·0.5H<sub>2</sub>O) C, H, N.

**2-(3-(Cyclopentyloxy)-4-methoxyphenyl)-5-ethoxy-2-(pyrid-4-ylmethyl)indan-1,3-dione (21).** Compound **21** was prepared similarly using conditions above: 33% yield; yellow solid; mp 60–65 °C; MS *m/z* 472 (M<sup>+</sup> + 1). Anal. Calcd for C<sub>29</sub>H<sub>29</sub>NO<sub>5</sub>: C, 73.87; H, 6.2; N, 2.97. Found: C, 73.25; H, 6.19; N, 2.83.

**[2-(3-(Cyclopentyloxy)-4-methoxyphenyl)-1,3-dioxo-2-(pyrid-4-ylmethyl)indan-5-yl]acetic Acid Trifluoroacetic Acid Salt (23).** A suspension of **20** (300 mg, 0.68 mmol), *tert*-butyl bromoacetate (0.1 mL, 0.68 mmol), and sodium hydride (28 mg, 60%, 0.68 mmol) in 10 mL of THF was refluxed for 2 h. The residue, after being filtered and concentrated, was purified by chromatography on silica gel (ether) to give 190 mg (50%) of the alkylated product: yellow solid; mp 51–54 °C; MS *m/z* 516 (M<sup>+</sup>).

A mixture of the alkylated product (180 mg) and TFA (1.5 mL) in 10 mL of methylene chloride was stirred at room temperature for 3 h. The residue obtained by concentration was purified by chromatography on silica gel (5% methanol/ethyl acetate) to give 100 mg (47%) as the trifluoroacetic acid salt: yellow solid; hygroscopic; mp 126–131 °C; MS *m/z* 501 (M<sup>+</sup>); <sup>1</sup>H NMR (CDCl<sub>3</sub>) δ 8.4 (bs, 1H), 7.81 (bd, 2H), 7.45–7.18 (bm, 5H), 7.05 (s, 1H), 6.90 (bd, 1H), 6.78 (d, 1H), 4.73 (bm, 3H), 3.79 (s, 3H), 3.57 (bd, 2H), 2.05–1.55 (bm, 8H). Anal. (C<sub>29</sub>H<sub>27</sub>NO<sub>7</sub>·C<sub>2</sub>HF<sub>3</sub>O<sub>2</sub>·2H<sub>2</sub>O) C, H, N.

**2-(3-(Cyclopentyloxy)-4-methoxyphenyl)-5-(1-methylpiperidin-4-yloxy)-2-(pyrid-4-ylmethyl)indan-1,3-dione (24).** Compound **24** was prepared similarly to **22**: 34.3% yield; yellow solid; hygroscopic; mp 67–72 °C; MS *m/z* 541 (M<sup>+</sup> + 1). Anal. (C<sub>33</sub>H<sub>36</sub>N<sub>2</sub>O<sub>5</sub>·H<sub>2</sub>O) C, H, N.

**2-(3-(Cyclopentyloxy)-4-methoxyphenyl)-1,3-dioxo-2-(pyrid-4-ylmethyl)indan-5-yl [1,4'-Bipiperidinyl-1'-carboxylate (25).** A mixture of **20** (215 mg, 0.49 mmol), [1,4'-bipiperidinyl-1'-carbonyl chloride [generated in situ from 4-piperidinopiperidine (370 mg, 2.2 mmol) and phosgene/toluene (1.93 M, 3.0 mL, 5.8 mmol)], and pyridine (0.1 mL) in 5 mL of THF was stirred overnight at room temperature before being diluted with ether (20 mL) and then filtered. The residue after concentration was purified by chromatography on silica gel (ethyl acetate) to give 100 mg (32%) of the desired product: yellow solid; hygroscopic; mp 75–78 °C; MS *m/z* 638 (M<sup>+</sup> + 1). <sup>1</sup>H NMR (CDCl<sub>3</sub>) δ 8.31 (bd, 2H), 7.89 (d, *J* = 8.4 Hz, 1H), 7.62 (bd, 1H), 7.5 (bd, 1H), 7.09 (d, *J* = 2.2 Hz, 1H), 7.02 (d, *J* = 5.5 Hz, 2H), 6.92 (dd, *J* = 2.2, 8.3 Hz, 1H), 6.76 (d, *J* = 8.7 Hz, 1H), 4.77 (m, 1H), 4.36 (m, 2H), 3.80 (s, 3H), 3.48 (s, 2H), 2.90 (m, 3H), 2.35–2.15 (m, 2H), 2.0–1.63 (bm, 10H). Anal. (C<sub>38</sub>H<sub>43</sub>N<sub>3</sub>O<sub>6</sub>·2.5H<sub>2</sub>O) C, H, N.

**Biological Methods. Preparation of PDE from Guinea Pig Macrophages.** The method of Turner et al.<sup>17</sup> was used. Briefly, cells were harvested from the peritoneal cavity of horse serum-treated (0.5 mL ip) Dunkin Hartley guinea pigs (250–400 g), and the macrophages were purified by discontinuous (55%, 65%, 70%, v/v) gradient (Percoll) centrifugation. Washed macrophages were plated out in cell culture flasks and allowed to adhere. The cells were washed with Hank's balanced salt solution, scraped from the flasks, and centrifuged (1000g). The supernatant was removed, and the pellets were stored at –80 °C until used. The pellet was homogenized in 20 mM tris-(hydroxymethyl)aminomethane HCl, pH 7.5, 2 mM MgSO<sub>4</sub>, 1 mM dithiothreitol, 5 mM ethylenediaminetetraacetic acid, 0.25 mM sucrose, 20 μM *p*-tosyl-L-lysine chloromethyl ketone, 10 μg/mL leupeptin, and 2000 U/mL aprotinin.

**Measurement of PDE Activity.** PDE activity was determined in macrophage homogenates by the two-step radioisotopic method of Thompson et al.<sup>18</sup> The reaction mixture contained 20 mM tris-(hydroxymethyl)aminomethane HCl (pH 8.0), 10 mM MgCl<sub>2</sub>, 4 mM 2-mercaptoethanol, 0.2 mM ethylenbis(oxyethylenenitrilo)tetraacetic acid, and 0.05 mg of bovine serum albumin/mL. The concentration of the substrate was 1 μM. The IC<sub>50</sub> values (i.e., concentrations which produce

50% inhibition of substrate hydrolysis) for the compounds examined were determined from concentration–response curves in which concentrations ranged from 0.1 nM to 10 μM. At least three concentration–response curves were generated for each agent, and **2** was used as control.

**Measurement of (+)-[<sup>3</sup>H]Rolipram Binding to Brain Membranes.** (±)-Rolipram was brominated in-house in CCl<sub>4</sub> (Mr. Kenneth Clow, Discovery Chemistry Department, Rhône-Poulenc Rorer) and subsequently tritiated by catalytic reduction with palladium and charcoal by Amersham International. The specific radioactivity of the (±)-[<sup>3</sup>H]rolipram was 24.7 Ci/mmol. Guinea pig brain membranes were prepared, and the binding assay was performed as described by Schneider et al.<sup>8b</sup> with (±)-[<sup>3</sup>H]rolipram (2 nM) and membrane samples corresponding to 500 μg of brain tissue.

**Canine Emesis Model.** Male and female beagle dogs (Marshall Farms, Rose, NY; 1–2 years of age, 8–10 kg) were used. Animals were fed once daily (in the morning) and given free access to water. Food was withheld the morning of a test. Compounds to be tested were dissolved in 100% DMSO. Compounds were administered intravenously into a cephalic vein (injection volume of 0.03 mL/kg) by slow bolus injection over a period of 30 s. Animals were monitored for emesis for up to 2 h or until emesis occurred. For a typical test, a total of 4 dogs (2 male, 2 female) were used.

**Murine Endotoxemia Model.** The ability of the test compounds to inhibit TNF-α production in vivo was evaluated in a mouse endotoxemia (i.e., lipopolysaccharide (LPS) challenge) model. Male, Balb/c mice (20–25 g; Harlan Sprague–Dawley Inc., Indianapolis, IN) were used. Test compounds were administered orally in a vehicle of 0.25% methylcellulose/0.2% Tween-20 in water 4 h prior to LPS challenge. Mice were then challenged with LPS (*Escherichia coli* 055:B5; Sigma Chemical Co., St. Louis, MO) at a dose of 30 μg/mouse by intraperitoneal injection. Ninety minutes following LPS injection, mice were anesthetized with isoflurane, and blood was collected by cardiac puncture. The whole blood was allowed to clot on ice, and serum was prepared by centrifugation at 500g for 10 min. Serum was assayed for TNF-α by ELISA (Genzyme Corp., Cambridge, MA).

**Molecular Modeling.** Computational approach was used to obtain low-energy conformations for **2**, **4**, **9**, and **14**. The initial molecular structures were constructed using Sybyl 6.3 (from Tripos Inc., 1699 S. Hanley Rd, St. Louis, MO 63144) by systematically rotating all three relevant torsion angles between the two aromatic rings. The amide bond was included to ensure the coverage of the conformational space. To avoid transition states and to allow more conformational space to be searched, the starting torsion angles of 45°, 135°, –45°, and –135° were assigned to those rotatable bonds. After an initial molecular mechanics optimization, a full geometric optimization was carried out for each of those initial conformations using MOPAC/AM1 6.00 (distributed by Tripos Inc., also available from Quantum Chemistry Program Exchange, Department of Chemistry, Indiana University, Bloomington, IN 47405). For low-energy conformations identified by geometric optimization, frequency calculations were performed to ensure that no negative second-derivative exists.

Several low-energy conformations were identified for **2**. The lowest-energy conformation was in a group of four conformations within an energy range of 1.0 kcal/mol. Two other conformations were located about 1.5 and 4.5 kcal/mol above the lowest-energy conformation. For indan **4**, a group of five conformations carried an energy close to one another. The lowest-energy conformation was 0.77, 0.95, 1.05, and 1.18 kcal/mol more stable than the rest of four conformations in the group, respectively. Another conformation was identified with an energy of 3.18 kcal/mol higher than that of the lowest-energy conformation.

## References

- Beutler, B.; Cerami, A. Cachectin and tumor necrosis factor as two sides of the same biological coin. *Nature* **1986**, *320*, 584–589.

- (2) (a) Strieter, R. M.; Remick, D. G.; Ward, P. A.; Spengler, R. N.; Lynch, J. P.; Larrick, J.; Kunkel, S. L. Cellular and molecular regulation of tumor necrosis factor- $\alpha$  production by pentoxifylline. *Biochem. Biophys. Res. Commun.* **1988**, *155*, 1230–1236. (b) Taffet, S. M.; Singhel, K. J.; Overholzer, J. F.; Shurtleff, S. A. Regulation of tumor necrosis factor expression in a macrophage-like cell line by lipopolysaccharide and cyclic AMP. *Cell. Immunol.* **1989**, *120*, 291–300.
- (3) (a) Duplantier, A. J.; Cheng, J. B. Emerging opportunities in the treatment of asthma and allergy. *Annu. Rep. Med. Chem.* **1994**, *29*, 73–81. (b) Nicholson, C. D.; Shahid, M. Inhibitors of cyclic nucleotide phosphodiesterase isozymes—their potential utility in the therapy of asthma. *Pulmonary Pharmacol.* **1994**, *7*, 1–17. (c) Torphy, T. J.; Livi, G. P.; Christensen, S. B. Novel phosphodiesterase inhibitors for the therapy of asthma. *Drug News Perspect.* **1993**, *6*, 203–214. (d) Lowe, J. A., III; Cheng, J. B. The PDE IV family of calcium-independent phosphodiesterase enzymes. *Drugs Future* **1994**, *29*, 73–81. (e) Palfreyman, M. N.; Souness, J. E. Phosphodiesterase type IV inhibitors. *Prog. in Med. Chem.* **1996**, *33*, 1–52.
- (4) Schwabe, U.; Miyake, M.; Ohga, Y.; Daly, J. 4-(3-Cyclopentyl-4-methoxyphenyl)-2-pyrrolidone (ZK62711): A potent inhibitor of adenosine cyclic 3',5'-monophosphate phosphodiesterase in homogenates and tissue slices from rat brain. *Mol. Pharmacol.* **1976**, *28*, 900–910.
- (5) Zeller, E.; Stief, H. J.; Pflug, B.; Satre, Y.; Hernandez, M. Results of a phase II study of the antidepressant effect of rolipram. *Pharmacopsychiatry* **1984**, *17*, 188–190.
- (6) (a) Ashton, M. J.; Cook, D. C.; Fenton, G.; Karlsson, J. A.; Palfreyman, M. N.; Raeburn, D.; Ratcliffe, A. J.; Souness, J. E.; Thurairatnam, S.; Vicker, N. Selective type IV phosphodiesterase inhibitors as antiasthmatic agents. The syntheses and biological activities of 3-(cyclopentyl)-4-methoxybenamides and analogues. *J. Med. Chem.* **1994**, *37*, 1696–1703. (b) Duplantier, A. J.; Biggers, M. S.; Chambers, R. J.; Cheng, J. B.; Cooper, K.; Damon, D. B.; Egger, J. F.; Kraus, K. G.; Marfat, A.; Masmune, H.; Pillar, J. S.; Shirley, J. T.; Umland, J. P.; Watson, J. W. Biarylcarboxylic acids and amides: inhibition of phosphodiesterase type IV versus [ $^3$ H]rolipram binding activity and their relationship to emetic behavior in the ferret. *J. Med. Chem.* **1996**, *39*, 120–125. (c) Masmune, H.; Cheng, J. B.; Cooper, K.; Egger, J. F.; Marfat, A.; Marshall, S. C.; Shirley, J. T.; Tickner, J. E.; Umland, J. P.; Vazquez, E. Discovery of micromolar PDE IV inhibitors that exhibit much reduced affinity for the [ $^3$ H]-rolipram binding site: 3-norbornyl-4-methoxyphenylmethylene oxindoles. *Bioorg. Med. Chem. Lett.* **1995**, *5*, 1965–1968. (d) Cheng, J. B.; Cooper, K.; Duplantier, A. J.; Egger, J. F.; Kraus, K. G.; Marshall, S. C.; Marfat, A.; Masmune, H.; Shirley, J. T.; Tickner, J. E.; Umland, J. P. Synthesis and in vitro profile of a novel series of catechol benimidazoles. The discovery of potent, selective phosphodiesterase type IV inhibitors with greatly attenuated affinity for the [ $^3$ H]rolipram binding site. *Bioorg. Med. Chem. Lett.* **1995**, *5*, 1969–1972. (e) Dal Piaz, V.; Giovannoni, M. P.; Castellana, C. Novel heterocyclic-fused pyridazinones as potent and selective phosphodiesterase IV inhibitors. *J. Med. Chem.* **1997**, *40*, 1417–1421. (f) Lampe, J. W.; Chou, Y.-L.; Hanna, R. G.; Di Meo, S. V.; Erhardt, P. W.; Hagedorn, A. A., III; Ingebretsen, W. R.; Cantor, E. (Imidazolylphenyl)pyrrol-2-one inhibitor of cardiac cAMP phosphodiesterase. *J. Med. Chem.* **1993**, *36*, 1041–1047. (g) Brackeen, M. F.; Cowan, D. J.; Stifford, J. A.; Schoenen, J. M.; Domanico, P. L.; Rose, D.; Strickland, A. B.; Vergheze, M.; Feldman, P. L. Design and synthesis of conformationally constrained analogues of 4-(3-butoxy-4-methoxy)imidazolidin-2-one (Ro 20-1724) as potent inhibitors of cAMP-specific phosphodiesterase. *J. Med. Chem.* **1995**, *38*, 4848–4854.
- (7) (a) Muller, T.; Engels, P.; Fozard, J. R. Subtypes of the type 4 cAMP phosphodiesterase: structure, regulation and selective inhibition. *Trends Pharmacol. Sci.* **1996**, *17*, 294–298. (b) Kelly, J. J.; Barnes, P. J.; Glembycz, M. A. Phosphodiesterase 4 in macrophages: relation between cAMP accumulation, suppression of cAMP hydrolysis and inhibition of [ $^3$ H]-(-)-rolipram binding by selective inhibitors. *Biochem. J.* **1996**, *318*, 425–436.
- (8) (a) Schmiechen, R.; Schneider, H. H.; Watchtel, H. Close correlation between behavioural response and binding in vivo for inhibitors of the rolipram-sensitive phosphodiesterase. *Psychopharmacology* **1990**, *102*, 17–20. (b) Schneider, H. H.; Schmiechen, R.; Brezinski, M.; Seidler, J. Stereospecific binding of the antidepressant rolipram to brain protein structures. *Eur. J. Pharmacol.* **1986**, *127*, 105–115. (c) Barnett, M. S.; O'Leary, B. J.; Burman, M.; Christensen, S. B.; Cieslinski, L. B.; Esser, K. M.; Prabhakar, U. S.; Rush, J. A.; Torphy, T. J. Association of the antiinflammatory activity of phosphodiesterase 4 (PDE4) inhibitors with either inhibition of PDE4 catalytic activity or competition for [ $^3$ H]rolipram binding. *Biochem. Pharmacol.* **1996**, *51*, 949–956. (d) Barnett, M. S.; Grous, M.; Cieslinski, L. B.; Burman, M.; Christensen, S. B.; Torphy, T. J. Inhibitors of phosphodiesterase IV (PDE IV) increase acid secretion in rabbit isolated gastric glands: correlation between function and interaction with a high-affinity rolipram binding site. *J. Pharmacol. Exp. Ther.* **1995**, *273*, 1396–1402.
- (9) (a) Warreilow, G. J.; Alexander, R. P.; Boyd, E. C.; Eaton, M. A.; Head, J. C.; Higgs, G. A. The design of an orally active PDE IV inhibitor (CDP 840) for asthma. 8th RSC–SCI Medicinal Chemistry Symposium, Cambridge, U.K., 1995. (b) Hughes, B. CDP 840. 2nd World Congress on Inflammation, Brighton, U.K., 1995. (c) Hughes, B. Fourth Annual Midwest Meeting of the Inflammation Research Association, Chicago, IL, 1996. (d) Hughes, B.; Howat, D.; Lisle, H. M.; James, T.; Gozzard, N.; Blease, K.; Hughes, P.; Kingaby, R.; Warreilow, G.; Alexander, R.; Head, J.; Boyd, E.; Eaton, M.; Perry, M.; Wales, M.; Smith, B.; Owens, R.; Catterall, C.; Lumb, S.; Russell, A.; Allen, R.; Merriman, M.; Bloxham, D.; Higgs, G. The inhibition of antigen-induced eosinophilia and bronchoconstriction by CDP840, a novel stereoselective inhibitor of phosphodiesterase type 4. *Br. J. Pharmacol.* **1996**, *118*, 1183–1191.
- (10) Unpublished results of Dagenham Research Centre, RPR, U.K.
- (11) Mitsunobu, O.; Yamada, M. Preparation of esters of carboxylic and phosphoric acid via quaternary phosphonium salts. *Bull. Chem. Soc. Jpn.* **1967**, *40*, 2380–2388.
- (12) Johnson, J. R. The Perkin reaction and related reactions. *Org. React.* **1942**, *1*, 211–256.
- (13) (a) Molnar-Kimber, K. L.; Yonno, L.; Heaslip, R. J.; Weichman, B. M. Differential regulation of TNF- $\alpha$  and IL-1 $\beta$  production from endotoxin stimulated human monocytes by phosphodiesterase inhibitors. *Mediat. Inflamm.* **1992**, *1*, 411–417. (b) Feldman, P. L.; Brackeen, M. F.; Cowan, D. J.; Marron, B. E.; Schoenen, F. J.; Stafford, J. A.; Suh, E. M.; Domanico, P. L.; Rose, D.; Leesnitzer, M. A.; Brawley, E. S.; Strickland, A. B.; Vergheze, M. W.; Connolly, K. M.; Bateman-Fite, R.; Noel, L. S.; Sekut, L.; Stimpson, S. A. Phosphodiesterase type IV inhibition. Structure–activity relationships of 1,3-disubstituted pyrrolidines. *J. Med. Chem.* **1995**, *38*, 1505–1510. (c) Souness, J. E.; Griffin, M.; Maslen, C.; Ebsworth, K.; Scott, L. C.; Pollock, K.; Palfreyman, M. N.; Karlsson, J.-A. Evidence that cyclic AMP phosphodiesterase inhibitors suppress TNF $\alpha$  generation from human monocytes by interacting with a 'low-affinity' phosphodiesterase 4 conformer. *Br. J. Pharmacol.* **1996**, *118*, 649–658.
- (14) For the therapeutic ratio of RP 73401 administered orally: Escott, K. J.; McMillan, S. J.; Birrell, M.; Webber, S. E.; Souness, J. E.; Maslen, C.; Temple, R.; Iqbal, S.; Mariucci, M.; Rose, J.; Geiger, L. E.; Thurairatnam, S.; Bower, S.; Aldous, D.; Sargent, C. A. Pharmacological profiling of phosphodiesterase 4 (PDE4) inhibitors and analysis of the therapeutic ratio in rats and dogs. *Br. J. Pharmacol.* **1998**, *123*, 40.
- (15) (a) Jezequel, S. G. Central nervous system penetration of drugs: importance of physicochemical properties. In *Progress in Drug Metabolism*; Gibson, G. G., Ed.; Taylor & Francis: London, U.K., 1992; Vol. 13, pp 141–178. (b) Lin, J. H.; Lu, A. Y. H. Role of pharmacokinetics and metabolism in drug discovery and development. *Pharmacol. Rev.* **1997**, *49*, 403–449.
- (16) Menard, M.; Erichomovitch, L.; La Brooy, M.; Chubb, F. L. Quelques metabolites possibles de la thalidomide. *Can. J. Chem.* **1963**, *41*, 1722–1724.
- (17) Turner, N. C.; Wood, L. J.; Burns, F. M.; Guerey, T.; Souness, J. E. The effect of cyclic AMP and cyclic GMP phosphodiesterase inhibitors on the superoxide burst of guinea-pig peritoneal macrophages. *Br. J. Pharmacol.* **1993**, *108*, 876–883.
- (18) Thompson, W. J.; Terasaki, W.; Epstein, P. M.; Strada, S. J. Assay of cyclic nucleotide phosphodiesterase and resolution of multiple molecular forms of the enzyme. *Adv. Cycl. Nucleotide Res.* **1979**, *10*, 69–92.

JM970575F